SUPPLEMENTARY MATERIAL: THE IMPACT OF CHANGES IN RESOLUTION ON THE PERSISTENT HOMOLOGY OF IMAGES

TERESA HEISS, SARAH TYMOCHKO, BRITTANY STORY, ADÈLIE GARIN, HOA BUI, BEA BLEILE, AND VANESSA ROBINS

1. Tighter Bounds

As mentioned in [2, Remark IV.10], the bound on the bottleneck distance in [2, Corollary IV.9] can be tightened from $3\sqrt{d}r$ to $2\sqrt{d}r$. To prove this, we first need to prove the tighter version of [2, Lemma IV.3] mentioned in [2, Remark IV.4]:

Lemma 1.1. *Let $A \subseteq \mathbb{R}^d$ have boundary with positive reach, and let $B \subseteq \mathbb{R}^d$.*
If $\max\{d_{\mathcal{H}}(A,B), d_{\mathcal{H}}(A^c,B^c)\} < reach(\partial A)$, then

$$\left\|d_A^{\mp} - d_B^{\mp}\right\|_{\infty} \leqslant \max\{d_{\mathcal{H}}(A,B),\ d_{\mathcal{H}}(A^c,B^c)\}.$$

Proof. Similarly to the proof of [2, Lemma IV.3], we distinguish between 4 different cases for an arbitrary point p. Cases 1 and 2 stay unchanged.

Case 3: $p \in A,\ p \notin B$. As in the proof of [2, Lemma IV.3], we need to bound $|d_A^{\mp}(p) - d_B^{\mp}(p)| = |-d(A^{\mathrm{c}},p) - d(p,B)| = d(A^{\mathrm{c}},p) + d(p,B)$. We distinguish between two sub-cases.

Case 3a: $p \in \partial A \cap A,\ p \notin B$. Then, $|d_A^{\mp}(p) - d_B^{\mp}(p)| = d(A^{\mathrm{c}},p) + d(p,B) \leqslant 0 + d_{\mathcal{H}}(A,B) \leqslant \max\{d_{\mathcal{H}}(A,B),\ d_{\mathcal{H}}(A^{\mathrm{c}},B^{\mathrm{c}})\}$.

Case 3b: $p \in \mathrm{int}(A),\ p \notin B$. Let $a \in \partial\,\mathrm{cl}(A^{\mathrm{c}})$ be such that $d(A^{\mathrm{c}},p) = d(\mathrm{cl}(A^{\mathrm{c}}),p) = d(a,p)$. As $a \neq p$, the vector $p-a$ has non-zero length. From $d(\mathrm{cl}(A^{\mathrm{c}}),p) = d(a,p)$ follows that $n_a = \frac{p-a}{\|p-a\|}$ is a unit normal vector of $\mathrm{cl}(A^{\mathrm{c}})$ at x (for a rigorous definition of normal vector, see [2, Definition A.2]). Let $\varepsilon \in (0, \mathrm{reach}(\partial A) - d_{\mathcal{H}}(A^{\mathrm{c}},B^{\mathrm{c}}))$. Let $x = a + (d_{\mathcal{H}}(A^{\mathrm{c}},B^{\mathrm{c}}) + \varepsilon)n_a$. As $d_{\mathcal{H}}(A^{\mathrm{c}},B^{\mathrm{c}}) + \varepsilon < \mathrm{reach}(\partial A) \leqslant \mathrm{reach}(\mathrm{cl}(A^{\mathrm{c}}))$, [2, Lemma A.3] yields $d(A^{\mathrm{c}},x) = d(\mathrm{cl}(A^{\mathrm{c}}),x) = d(a,x) = d_{\mathcal{H}}(A^{\mathrm{c}},B^{\mathrm{c}}) + \varepsilon > d_{\mathcal{H}}(A^{\mathrm{c}},B^{\mathrm{c}})$. Hence, by the definition of Hausdorff distance, x cannot be in B^{c} and thus $x \in B$. The points a,p,x lie on a straight line by construction. To prove $d(a,p) < d(a,x)$, let us assume $d(a,p) \geqslant d(a,x)$ getting a contradiction from $d(A^{\mathrm{c}},p) = d(a,p) \geqslant d(a,x) > d_{\mathcal{H}}(A^{\mathrm{c}},B^{\mathrm{c}})$ and $p \in B^{\mathrm{c}}$. Therefore, p lies on the line segment between a and x. With this we can bound $d(A^{\mathrm{c}},p) + d(p,B) \leqslant d(a,p) + d(p,x) = d(a,x) = d_{\mathcal{H}}(A^{\mathrm{c}},B^{\mathrm{c}}) + \varepsilon$. As this bound is true for every $\varepsilon \in (0, \mathrm{reach}(A^{\mathrm{c}}) - d_{\mathcal{H}}(A^{\mathrm{c}},B^{\mathrm{c}}))$, we follow $|d_A^{\mp}(p) - d_B^{\mp}(p)| = d(A^{\mathrm{c}},p) + d(p,B) \leqslant d_{\mathcal{H}}(A^{\mathrm{c}},B^{\mathrm{c}}) \leqslant \max\{d_{\mathcal{H}}(A,B),\ d_{\mathcal{H}}(A^{\mathrm{c}},B^{\mathrm{c}})\}$.

Case 4: $p \notin A,\ p \in B$. Analogously $|d_A^{\mp}(p) - d_B^{\mp}(p)| \leqslant \max\{d_{\mathcal{H}}(A,B),\ d_{\mathcal{H}}(A^{\mathrm{c}},B^{\mathrm{c}})\}$. □

With this we can proof the tighter version of [2, Corolary IV.9], mentioned in [2, Remark IV.10]:

Corollary 1.2. *Using the notation of [2, Theorem IV.1]. If $r < \frac{1}{\sqrt{d}} reach(\partial X)$, then*

$$\mathrm{d_B}(\mathrm{PD}\left(d_X^{\mp}\right), \mathrm{PD}\left(D_r\right)) \leqslant 2\sqrt{d}r$$

Proof. Note that $\max\{d_{\mathcal{H}}(X,X(r,t)),\ d_{\mathcal{H}}(X^{\mathrm{c}},X(r,t)^{\mathrm{c}})\}$ is the maximum of the 4 suprema from [2, Lemma IV.7]. We thus use [2, Lemma IV.7] to bound $\max\{d_{\mathcal{H}}(X,X(r,t)),\ d_{\mathcal{H}}(X^{\mathrm{c}},X(r,t)^{\mathrm{c}})\}$ by $\max\{l_X(\sqrt{d}r), \sqrt{d}r\}$, which is $\sqrt{d}r$ by [2, Lemma IV.8].

Similarly to the proof of [2, Lemma IV.6], we combine the stability theorem of persistent homology [1], the triangle inequality, and [2, Lemma IV.2], now with the new Lemma 1.1:

$$\begin{aligned}
&\mathrm{d_B}(\mathrm{PD}\left(d_X^{\mp}\right), \mathrm{PD}\left(D_r\right)) \\
&\leqslant \left\| d_X^{\mp} - D_r \right\|_\infty \\
&\leqslant \left\| d_X^{\mp} - d_{X(r,t)}^{\mp} \right\|_\infty + \left\| d_{X(r,t)}^{\mp} - D_r \right\|_\infty \\
&\leqslant \max\{d_{\mathcal{H}}(X, X(r,t)),\ d_{\mathcal{H}}(X^{\mathrm{c}}, X(r,t)^{\mathrm{c}})\} + \sqrt{d}r \\
&\leqslant 2\sqrt{d}r.
\end{aligned}$$

□

2. Persistence Diagrams from Material Science Examples

Section V.B in [2] presents three material science examples: glass bead packing, a Castlegate sandstone sample and a sand packing sample. The original binary images are available from [4]. In Figures. 1, 2 and 3, we show the computed persistence diagrams for the 3D images with several resolutions for the bead packing, castlegate sandstone and sand packing, respectively.

As shown in [3], the percolation threshold, l_c, can be determined from the distribution of points in the zero dimensional persistence diagram. This threshold is the radius of the largest sphere that can pass through the pore space from one side of the image to the opposite and is an important physical parameter associated with porous materials.

In the three sets of examples shown in Figures 1-3, the distribution of points in $\mathrm{PD}\,(0)\,D_n$ shows a clear signature of this critical length scale. This signature yields the same estimate for l_c for image resolutions $n = 512, 256, 128$ in the three example materials.

Acknowledgements

The authors want to thank Mathijs Wintraecken for the idea of tightening the bounds when the Hausdorff distance is below the reach, i.e. the idea for Lemma 1.1.

References

[1] David Cohen-Steiner, Herbert Edelsbrunner, and John Harer. Stability of persistence diagrams. *Discrete & computational geometry*, 37(1):103–120, 2007.

[2] Teresa Heiss, Sarah Tymochko, Brittany Story, Adèlie Garin, Hoa Bui, Bea Bleile, and Vanessa Robins. The impact of changes in resolution on the persistent homology of images. *In Submission*, 2021.

[3] Vanessa Robins, Mohammad Saadatfar, Olaf Delgado-Friedrichs, and Adrian P. Sheppard. Percolating length scales from topological persistence analysis of micro-CT images of porous materials. *Water Resources Research*, 52(1):315–329, January 2016.

[4] Adrian Sheppard and Masa Prodanovic. Network generation comparison forum. `http://www.digitalrocksportal.org/projects/16`, 2015.

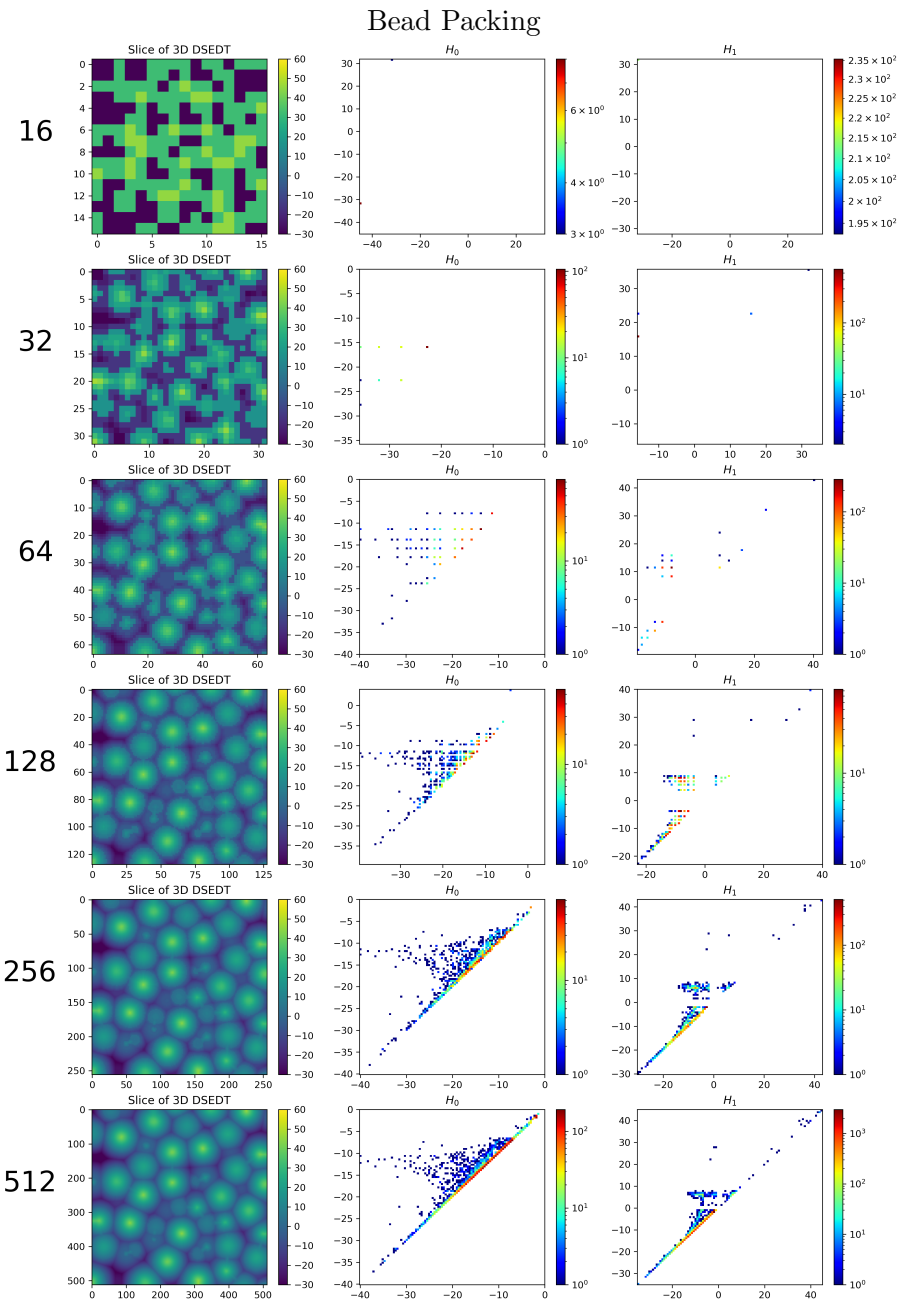

FIGURE 1. Each row shows a slice of the 3D SEDT, and the 0 and 1 dimensional persistence diagrams of the bead packing sample at many resolutions.

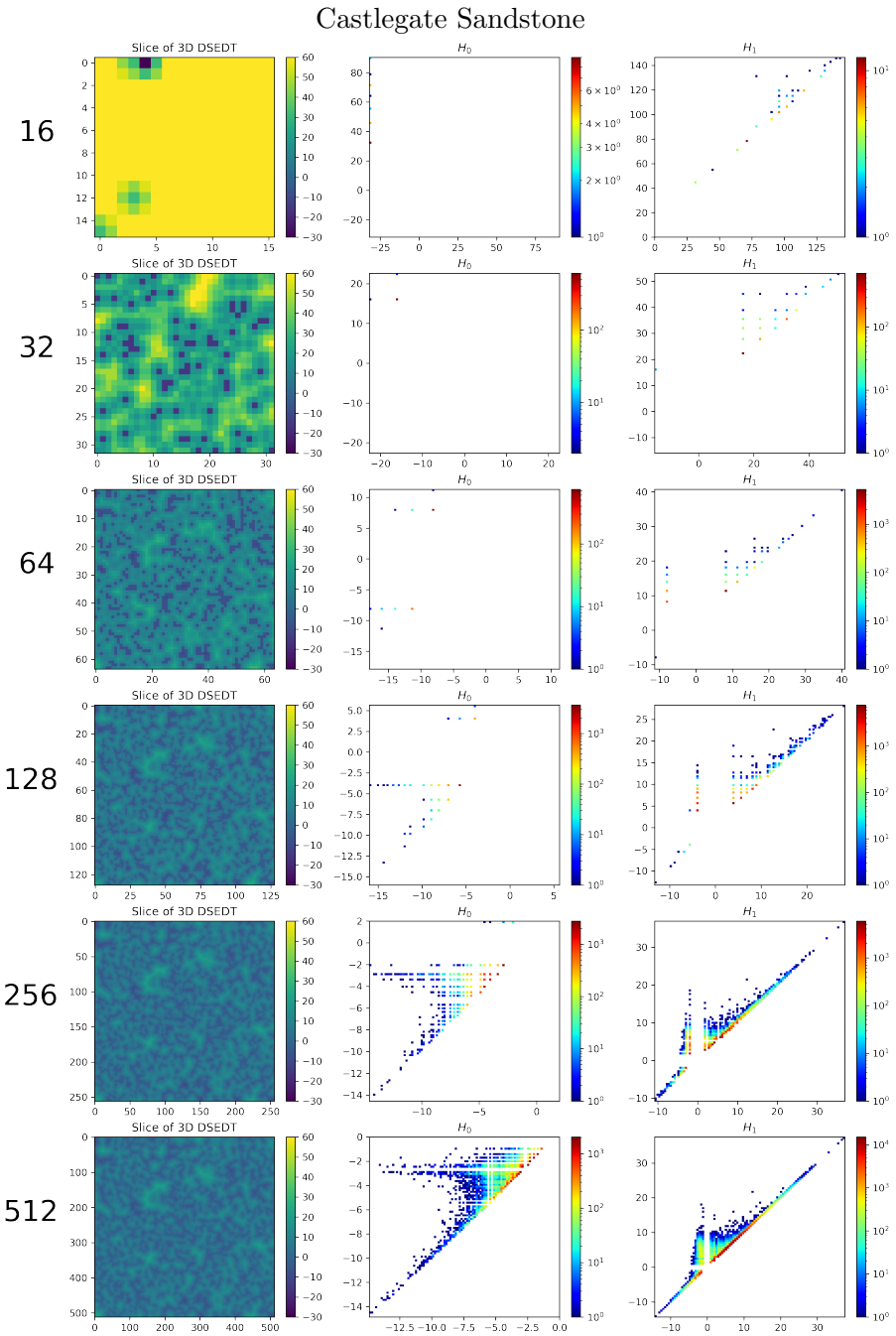

FIGURE 2. Each row shows a slice of the 3D SEDT, and the 0 and 1 dimensional persistence diagrams of the castlegate sandstone sample at many resolutions.

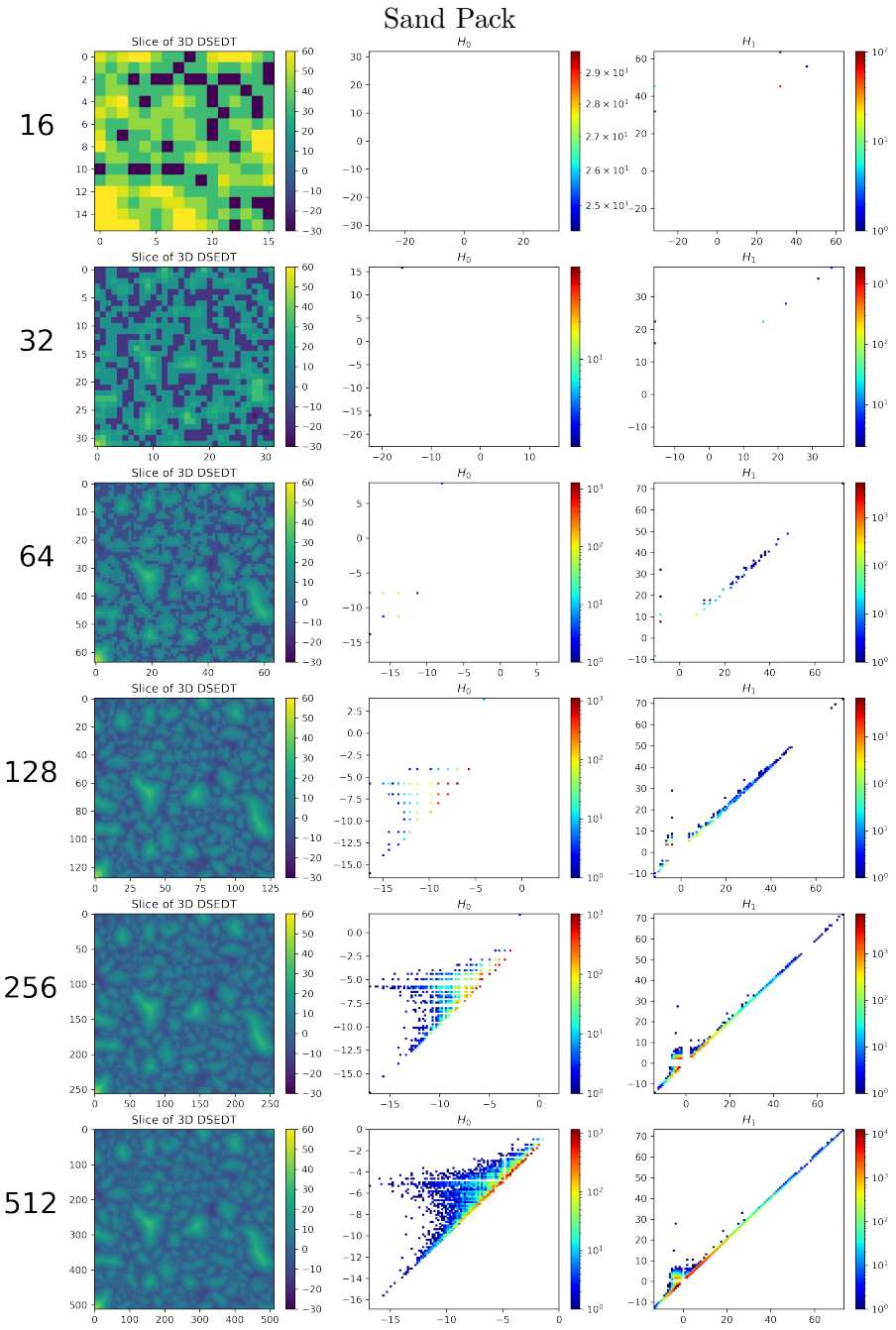

FIGURE 3. Each row shows a slice of the 3D SEDT, and the 0 and 1 dimensional persistence diagrams of the sand packing sample at many resolutions.